Electron transmission dynamics of $Ge_{1-x}Sn_x$ alloys based on inter-valley electrons transferring effect*

HUANG Shihao, LI Jiapeng, LI Hailin, LU Xuxing, SUN Qinqin, XIE Deng
School of Electronic, Electrical Engineering and Physics, Fujian University of Technology, Fuzhou 350118, China

Abstract

$Ge_{1-x}Sn_x$ alloys have aroused great interest in silicon photonics because of their compatibility with complementary metal-oxide-semiconductor (CMOS) technology. As a result, they are considered potential candidate materials. Owing to the significant differences in effective mass within the valleys, the unique dual-valley structure of Γ valley and L valley in energy can improve the optoelectronic properties of $Ge_{1-x}Sn_x$ alloys. Therefore, inter-valley scattering mechanisms between the Γ and L valley in $Ge_{1-x}Sn_x$ alloys are crucial for understanding the electronic transports and optical properties of $Ge_{1-x}Sn_x$ materials. This work focuses on the theoretical analysis of inter-valley scattering mechanisms between Γ and L valley, and hence on the electron transmission dynamics in $Ge_{1-x}Sn_x$ alloys based on the phenomenological theory model. Firstly, the 30th-order $k\ p$ perturbation theory is introduced to reproduce the band structure of $Ge_{1-x}Sn_x$. The results show that the effective mass of L valley is always about an order of magnitude higher than that of Γ valley, which will significantly influence the electron distributions between Γ and L valley. Secondly, the scattering mechanism is modeled in $Ge_{1-x}Sn_x$ alloys. The results indicate that scattering rate $R_{\Gamma L}$ is about an order of magnitude higher than $R_{L\Gamma}$, while $R_{\Gamma L}$ decreases with the increase of Sn composition and tends to saturate when Sn component is greater than 0.1. And $R_{L\Gamma}$ is almost independent of the Sn component. Thirdly, kinetic processes of carriers between Γ and L valley are proposed to analyze the electron transmission dynamics in $Ge_{1-x}Sn_x$ alloys. Numerical results indicate that the electron population ratio for Γ-valley increases and then tends to saturation with the increase of Sn composition, and is independent of the injected electron concentration. The model without the scattering mechanism indicates that the electron population ratio for Γ-valley in indirect-$Ge_{1-x}Sn_x$ alloys is independent of the injected electron concentration, while the electron population ratio for Γ-valley in direct-$Ge_{1-x}Sn_x$ alloys is dependent on the injected electron concentration, and the lower the electron concentration, the greater the electron population ratio for Γ-valley is. The results open a new way of understanding the mechanisms of electron mobility, electrical transport, and photoelectric conversion in $Ge_{1-x}Sn_x$ alloys, and can provide theoretical value for designing $Ge_{1-x}Sn_x$ alloys in the fields of microelectronics and optoelectronics.

Keywords: $Ge_{1-x}Sn_x$ alloys, electron-phonon interaction, inter-valley scattering model
PACS：61.66.Dk, 63.20.kd, 05.45.Mt
doi: 10.7498/aps.74.20240980

* The paper is an English translated version of the original Chinese paper published in *Acta Physica Sinica*. Please cite the paper as: HUANG Shihao, LI Jiapeng, LI Hailin, LU Xuxing, SUN Qinqin, XIE Deng; Electron transmission dynamics of $Ge_{1-x}Sn_x$ alloys based on inter-valley electrons transferring effect. *Acta Physica Sinica* 2025, 74(3): 036101. doi: 10.7498/aps.74.20240980

cstr: 32037.14.aps.74.20240980

1. Introduction

$Ge_{1-x}Sn_x$ materials have not only unique electronic and optical properties, but also compatible with Si based CMOS process. They are one of the hot research materials in Si based microelectronics and optoelectronics[1,2]. On the one hand, $Ge_{1-x}Sn_x$ are ideal materials for Si-based high mobility devices because of their high carrier mobility[3,4]. On the other hand, its response band covers the near-infrared to mid-infrared band, and it is one of the candidate materials for the preparation of Si-based high-performance infrared detectors[5,6]. At the same time, $Ge_{1-x}Sn_x$ has the characteristic of tunable band structure. When the Sn composition reaches about 0.07, $Ge_{1-x}Sn_x$ can be modulated into a direct band gap material, which is considered to be the most promising material for Si-based lasers[7–9]. Therefore, $Ge_{1-x}Sn_x$ have broad application prospects in the fields of electronics, detection and luminescence[10–13].

Carrier dynamics plays an important role in the performance of semiconductor optoelectronic devices. In reference [14], the effect of the separation of the Γ and L valley electrons due to the momentum k space on the performance of $Ge_{1-x}Sn_x$ photodetectors was theoretically analyzed. However, the energy gap between the direct band and the indirect band of $Ge_{1-x}Sn_x$ is small, and there are few reports on the scattering of electrons between the two valleys. The intervalley scattering work of Ge materials in references [15,16] shows that under the scattering effect of intervalley phonons, both strain and N-type doping can effectively improve the filling rate of conduction band direct band Γ energy valley electrons, thereby improving the direct band luminescence efficiency of Ge.

Experimentally, the microscopic behavior of electron-phonon interaction in materials can be observed by time-resolved angle-resolved photoelectron spectroscopy, time-resolved X-ray scattering free electron laser, and time-resolved electron diffraction spectroscopy[17–19]. For example, reference [17] directly observed the intervalley scattering behavior of Ge material through X-ray free electron laser experiments, and found that the intervalley scattering time of Ge material is in the order of picoseconds (ps). However, due to the lack of a time-resolved spectrometer suitable for narrow band gap materials, there are few reports on the direct observation of intervalley scattering effects of $Ge_{1-x}Sn_x$. In the literature, the carrier lifetime is often measured by photoluminescence spectroscopy and photoconductivity measurement, and then the intervalley scattering behavior of $Ge_{1-x}Sn_x$ is indirectly inferred from the physical model[20,21]. For example, in reference [21], the intervalley scattering time of the energy valley from Γ to L in the order of picoseconds was estimated in $Ge_{1-x}Sn_x$ by combining time-resolved reflectance spectroscopy and photoluminescence spectroscopy. Although these studies are helpful to understand the dynamic behavior of carriers and provide rational thinking for the design of $Ge_{1-x}Sn_x$ optoelectronic devices, the microscopic mechanism of $Ge_{1-x}Sn_x$ carrier intervalley transfer is far from being clarified.

In this paper, the intervalley phonon driven carrier dynamics in $Ge_{1-x}Sn_x$ is systematically discussed from the aspects of energy band structure characteristics, carrier distribution simulation, intervalley optical phonon scattering modeling, and intervalley electron transfer modeling. The results provide a theoretical reference for the application of $Ge_{1-x}Sn_x$ in the field of electronics and optoelectronics.

2. Modeling of intervalley electron transfer effect

Electrons move under the action of the periodic lattice potential field, and then form the electronic band structure. Phonons are formed by the vibration of the lattice, so the electrons are scattered by phonons in the process of motion. The dispersion relation of the band structure plays an important role in the energy conservation of electron-phonon interaction, and the strength of electron-phonon coupling affects the intervalley electron scattering rate of $Ge_{1-x}Sn_x$, so the band structure of materials is closely related to the carrier scattering. In this paper, the 30-band $k \cdot p$ model based on perturbation theory is used to calculate the dispersion characteristics[22,23] of the electronic structure of $Ge_{1-x}Sn_x$, and the relevant parameters are extracted from the band structure, including the electronic density of States effective mass and band gap of the conduction band direct band Γ and indirect band L valleys.

On the basis of band parameters, the distribution of electrons in the conduction band Γ and L valley of Ge_{1-x} Sn_x material can be expressed by (1):

$$n = \frac{1}{2\pi^2}\left(\frac{2k_BT}{\hbar^2}\right)^{3/2}\left\{\int_0^\infty \frac{m_n^L x^{1/2}\mathrm{d}x}{1+\exp(x-\xi)} + \int_0^\infty \frac{m_n^\Gamma x^{1/2}\mathrm{d}x}{1+\exp[x-\xi+(\frac{\Delta E_{\Gamma L}}{k_BT})]}\right\}, \tag{1}$$

Where k_B is the Boltzmann constant; The T is 300 K at room temperature; $\hbar$ is the reduced Planck constant; m_n^L and m_n^Γ are the density-of-state effective masses of the L valley and the Γ valley, respectively; $\xi = \frac{E_F - E_C}{k_BT}$, E_F are the Fermi level, and E_C is the conduction band minimum of the indirect band; $\Delta E_{\Gamma L}$ is the energy difference between the Γ valley and the L valley.

The intervalley scattering model of $Ge_{1-x}Sn_x$ material is shown as (2)[15]:

$$W_o(E_k) = \frac{\pi D_{\Gamma L}^2 N_{val}}{\rho\omega_{\Gamma L}}\left\{n(\omega_{\Gamma L})N(E) + [n(\omega_{\Gamma L})+1]N(E)\right\}, \tag{2}$$

Where:

$$N(E) = \frac{\left(2m_{\mathrm{d}}^{*}\right)^{3/2} E^{1/2}}{4\pi^{2}\hbar^{3}}, \tag{3}$$

$$E = E_{\mathrm{k}} \pm \Delta E_{\Gamma L} \pm \hbar\omega_{\Gamma L}, \tag{4}$$

$$m_{\mathrm{d}}^{*} = \left(m_{//}^{*} m_{\perp}^{*^{2}}\right)^{1/3}, \tag{5}$$

$$n(\omega_{\Gamma L}) = \left[\exp\left(\frac{\omega_{\Gamma L}}{k_{\mathrm{B}}T}\right) - 1\right]^{-1}. \tag{6}$$

In (2), the first term after the equal sign represents the transition process of absorbing intervalley optical phonons, the second term represents the transition process of emitting intervalley optical phonons, $N(E)$ is the energy density of States of the final valley of the transition, and $n(\omega_{\Gamma L})$ is the average phonon number. Where N_{val} is the number of isoenergetic valleys; ρ is that bulk density of the $Ge_{1-x}Sn_x$ material, and is the linear difference between the Ge and Sn material; $m_{//}^{*}, m_{\perp}^{*}$ represent that transverse and longitudinal effective masses of the conduction band L valley, respectively; Because there are few reports on the deformation parameter and angular frequency of the intervalley optical phonon of $Ge_{1-x}Sn_x$, and the composition of Sn calculated in this paper is x<0.2, which is low and close to that of Ge material, the relevant parameters of Ge are used to approximate the calculation process, that is, the deformation parameter and angular frequency of the intervalley optical phonon are $D_{\Gamma L}$ = 4 × 10^8 eV/cm and $\omega_{\Gamma L}$=4.11×1013 rad/s, respectively[24].

The scattering rate reflects the number of carrier scattering per unit time, and its expression is shown in (7):

$$P = \frac{\int_{0}^{\infty} f(E)\, E^{3/2} \mathrm{d}E}{\int_{0}^{\infty} \frac{f(E)}{W_{\mathrm{o}}(E)} E^{3/2} \mathrm{d}E}, \tag{7}$$

$$f(E) = \frac{1}{1 + \exp\left(\frac{E - E_{\mathrm{F}}}{k_{\mathrm{B}}T}\right)}, \tag{8}$$

Where $f(E)$ is the Fermi-Dirac distribution function.

Under the action of intervalley optical phonons, the distribution of electrons between the L valley and the Γ valley is shown in (9) and (10):

$$\frac{\mathrm{d}n_\Gamma}{\mathrm{d}t} = -R_{\Gamma L} \cdot n_\Gamma + R_{L\Gamma} \cdot n_L, \tag{9}$$

$$\frac{\mathrm{d}n_L}{\mathrm{d}t} = R_{\Gamma L} \cdot n_\Gamma - R_{L\Gamma} \cdot n_L, \tag{10}$$

Where $R_{L\Gamma}$ and $R_{\Gamma L}$ are the intervalley optical phonon scattering rates of the L valley to the Γ valley and the Γ valley to the L valley, respectively, and n_Γ and n_L are the carrier concentrations of the Γ valley and the L valley, respectively.

3. Results and Discussion

The band parameters of Ge_{1-x} Sn_x are shown in the Fig. 1. From the Fig. 1(a), it can be seen that the energy difference between the Γ valley and the L valley decreases linearly with the increase of Sn composition; When the Sn composition x = 0.07, the Ge_{1-x} Sn_x changes from an indirect band material to a direct band material, which is consistent with the experimental observation[25].

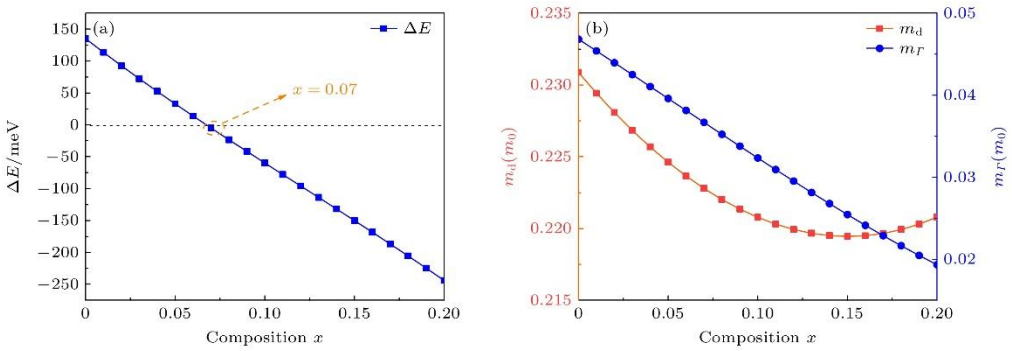

Figure 1. Parameters of Ge_{1-x} Sn_x: (a) The energy difference of Γ and L valley as a function of composition x; (b) the electron density of states (DOS) effective masses at Γ and L valley as a function of composition x.

The Fig. 1(b) shows the dependence of the conduction band electronic density of States on the Sn composition. The conduction band Γ valley density of electronic States effective mass decreases linearly with increasing Sn fraction. However, the effective mass of the electron density of States in the L of the conduction band varies quadratically with the increase of the Sn composition. When the x = 0.15, the effective mass of the electron density of States in the L valley reaches a minimum (m_d = 0.220m_0). Different from the traditional $Ge_{1-x}Si_x$ materials, theoretical and experimental studies have shown that the nonlinear extrapolation of the effective mass parameters in the $Ge_{1-x}Sn_x$ system has been proved to be reliable[23].

It is worth mentioning that the L valley-density-of-state effective mass is consistently about an order of magnitude higher than the Γ valley-density-of-state effective mass. This indicates that the injected electrons tend to fill in the indirect band L valley in the quasi-direct band gap $Ge_{1-x}Sn_x$ materials.

The calculated intervalley scattering rate of Ge_{1-x} Sn_x is shown in the Fig. 2. The Fig. 2(a) show that the Ge_{1-x} Sn_x material with low Sn composition (x< 0.07) is an indirect band material, and the energy of the electron in the Γ valley is higher than that of the indirect band L valley, so the

electron in the direct band Γ valley is easily scattered to the indirect band L valley through the emission of intervalley optical phonons. However, because Ge_{1-x} Sn_x with high Sn composition (x> 0.07) is a direct band material, the electron in the direct band Γ valley can not jump to the indirect band L valley by absorbing or emitting intervalley optical phonons only when it gains enough energy, and under a certain momentum supply.

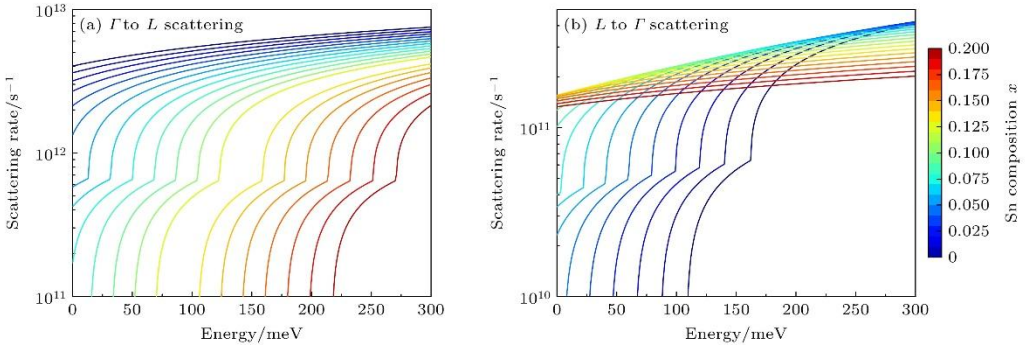

Figure 2. Inter-valley scattering rate (a) from Γ to L valleys and (b) from L to Γ valley with different Sn compositions.

The opposite is true for the case where the electron in the indirect band L valley scatters to the direct band Γ valley, as shown in the Fig. 2(b). The simulation results show that the electrons in the L valley of the indirect band Ge_{1-x} Sn_x material with low Sn composition can be scattered into the Γ valley by absorbing or emitting intervalley optical phonons only when they obtain high enough energy. However, for the Ge_{1-x} Sn_x material with high Sn composition, the energy of the electron in the L valley is higher than that in the direct band Γ valley, so the electron in the L valley can easily jump to the direct band Γ valley by emitting intervalley optical phonons.

It is worth mentioning that the higher the composition of the direct band Ge_{1-x} Sn_x materials, the more difficult the intervalley scattering of electrons in the Γ valley. However, most of the carriers in the indirect band Ge_{1-x} Sn_x materials with low Sn composition are scattered into the direct band Γ valley at room temperature only by overcoming the energy of $1kT$ — $3kT$, although most of the carriers are in the L valley. It can be seen from the qualitative analysis that the intervalley optical phonon scattering from the L valley to the Γ valley is more likely to occur in the Ge_{1-x} Sn_x material with low Sn composition.

In order to further quantitatively reveal the factors affecting the intervalley scattering, the relationship between the injected carriers and the intervalley scattering rate is calculated, as shown by Fig. 3. On the one hand, high injected carrier concentration can enhance the scattering rate of Ge_{1-x} Sn_x, which is consistent with the experimental observation of strong intervalley scattering from indirect band to direct band in n-type heavily doped Ge-on-Si materials reported in Ref[26]. On the other hand, the calculated average carrier scattering time of Ge material is 216 fs, which is in good agreement with the experimental average scattering time of bulk Ge (230 ± 25) fs and the average scattering time of Ge/SiGe quantum well system of 185 fs[27–29], further verifying the correctness of the calculated results in this paper.

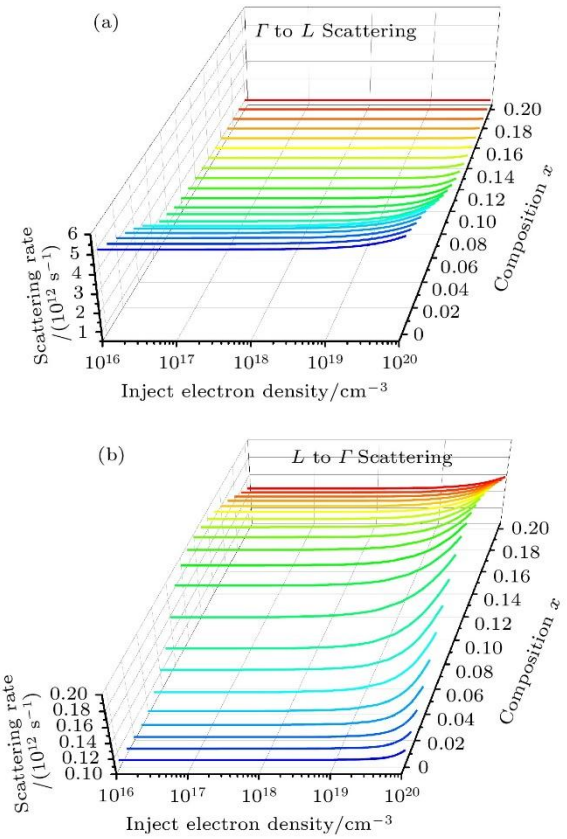

Figure 3. Relationship between inter-valley scattering rate and inject electron density under the condition of different Sn compositions: (a) From Γ to L valleys scattering; (b) from L to Γ valley scattering.

The relationship between the scattering rate of intervalley optical phonons and the Sn composition is shown in Fig. 4. The electron scattering rate from the Γ valley to the L valley decreases with the increase of Sn composition, and tends to saturate when the Sn composition is greater than 0.1. This is because the L valley has a large effective mass of the electron density of States, and for the direct band Ge_{1-x} Sn_x material with Sn composition less than 0.1, the difference between the direct band and the indirect band is small, and the electrons in the Γ valley can still be quickly scattered to the L valley through the intervalley scattering process. The scattering rate of electrons from the L valley to the Γ valley is almost unchanged with the change of Sn composition. At the same time, the electron scattering rate from the Γ valley to the L valley is about one order of magnitude higher than that from the L valley to the Γ valley. This is mainly because the effective mass of the L valley electron density of States is always about an order of magnitude higher than that of the Γ valley electron density of States.

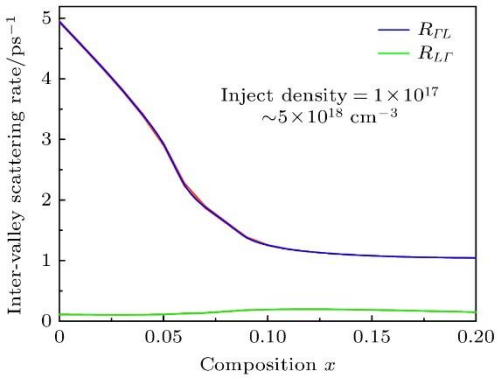

Figure 4. Inter-valley scattering rate from Γ to L valleys scattering and from L to Γ valley scattering under different Sn compositions.

The relationship between electron concentration in conduction band for Γ and L energy valley and intervalley electron transfer time of Ge_{1-x} Sn_x material is shown in the Fig. 5, and the inset is the linear coordinate. The results show that most of the initially injected electrons are distributed in the L valley for the indirect band Ge_{1-x} Sn_x materials with low Sn composition because the effective mass of the density of States in the L valley is larger than that in the direct band. However, with the participation of phonons, the electron concentration in the Γ valley increases rapidly after an average of about 0. 3 ps, while the electron concentration in the L valley does not decrease significantly. The results show that the intervalley electron transfer effect is beneficial to the increase of the electron concentration of the Γ valley in the indirect band Ge_{1-x} Sn_x materials with low Sn composition.

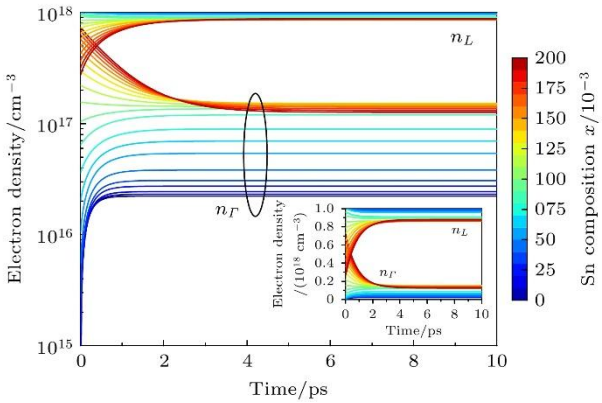

Figure 5. Relationship between electron transmission time and electron density in Γ, L valleys with various Sn compositions, the inset shows as a linear scale.

For the high Sn composition Ge_{1-x} Sn_x with direct band, most of the initially injected electrons are distributed in the Γ valley because the energy of the Γ valley is lower than that of the L valley. However, with the participation of phonons, the electron concentration in the Γ valley decreases slowly, while the electron concentration in the L valley increases slowly. The main reason for this phenomenon is that the effective mass of the electron density of States in the L valley is large.

The dependence of the constant for scattering time on the Sn composition is shown in Fig. 6. The results show that the constant for scattering time is prolonged with the increase of Sn content. That is to say, the lower the composition, the more favorable the electron-phonon interaction is for the

redistribution of intervalley electrons. From the point of view of luminescence, the effect of intervalley scattering is more conducive to the rapid replenishment of electrons from the *L* valley to the *Γ* valley in $Ge_{1-x}Sn_x$ materials with low Sn composition, thus improving the direct band luminescence efficiency.

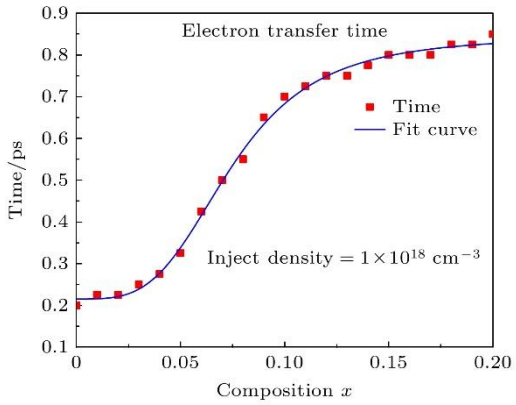

Figure 6. Relationship between composition and time-delay.

In order to further reveal the distribution of the injected electron concentration in the *Γ* and *L* valleys, the relationship between the electron filling fraction of the *Γ* valley and the *L* valley and the Sn composition is calculated under different injected electron concentrations, as shown in the Fig. 7. The calculation results show that when the Sn composition is to $x < 0.7$, compared with the case without considering the scattering model, the lower the composition is, the more significant the electron-phonon interaction is to improve the electron filling fraction of the direct band *Γ* valley, and the effect of scattering on the electron distribution is not related to the injected carrier concentration. When $0.7<x< 0.1$, the electron filling fraction of the direct band *Γ* valley increases with the increase of Sn composition considering the scattering model; However, without considering the scattering model, the higher the carrier concentration, the lower the electron filling fraction of the direct band *Γ* valley, because with the increase of the Fermi level, most of the electrons tend to distribute in the *L* valley with larger effective mass. When $x> 0.10$, $Ge_{1-x}Sn_x$ is a direct band material. Considering the scattering model, the Sn composition increases and the electron filling fraction of the direct band *Γ* valley tends to be saturated. However, without considering the scattering model, the electron filling fraction of the direct band *Γ* valley is related to the concentration of the injected carriers. For the same composition, the smaller the injected electron concentration is, the higher the electron filling fraction of the direct band *Γ* valley is, because the Fermi level is far away from the conduction band at low injected electron concentration, and the electrons preferentially occupy the *Γ* valley with lower energy level; When the injected electron concentration is high, the Fermi level is close to the *L* valley, and the effective mass of the *L* valley is larger than that of the *Γ* valley, so most of the electrons will be distributed in the *L* valley, resulting in a decrease in the electron filling fraction of the direct band *Γ* valley.

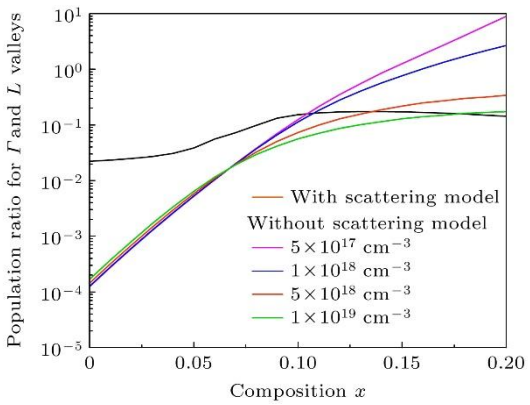

Figure 7. Simulated electron population ratio for Γ and L valleys as a function of Sn compositions, with and without the scattering model.

4. Conclusion

In this paper, the intervalley optical phonon scattering mechanism between the conduction band direct band Γ and the indirect band L valley of $Ge_{1-x}Sn_x$ is simulated and analyzed. The numerical results show that the electron scattering rate from the Γ valley to the L valley is higher than that from the L valley to the Γ valley because the effective mass of the electron density of States in the L valley of $Ge_{1-x}Sn_x$ is always about one order of magnitude higher than that in the Γ valley. At the same time, the scattering rate of electrons from the Γ valley to the L valley decreases with the increase of Sn composition, and tends to saturate when Sn composition is greater than 0.1. The scattering rate of electrons from the L valley to the Γ valley is almost unchanged with the change of Sn composition. In addition, the intervalley electron transfer model shows that the electron filling fraction of the direct band Γ energy has little to do with the injected electron concentration, and increases first and then tends to saturate with the increase of Sn composition. Without considering the scattering model, the higher the composition of the indirect band $Ge_{1-x}Sn_x$ material, the more beneficial it is to improve the electron filling fraction of the direct band Γ valley, and it has little to do with the injected carrier concentration; For the direct band $Ge_{1-x}Sn_x$ material, the electron filling fraction of the Γ valley is related to the injected electron concentration, and the lower the electron concentration is, the larger the electron filling fraction of the Γ valley is due to the fact that the Fermi level is far away from the conduction band minimum. The quantitative data are helpful to understand the microscopic mechanism of carrier scattering in Ge-Sn materials, and can provide theoretical reference value for the design of related materials and devices.

References

[1] Miao Y H, Wang G L, Kong Z Z, Xu B Q, Zhao X W, Luo X, Lin H X, Dong Y, Lu B, Dong L P, Zhou J R, Liu J B, Radamson H H 2021 Nanomaterials 11 2556

[2] Oka H, Mizubayashi W, Ishikawa Y, Uchida N, Mori T, Endo K 2021 Appl. Phys. Express 14 096501

[3] Zhang D, Song J J, Xue X X, Zhang S Q 2022 Chin. Phys. B 31 068401

[4] Wang H J, Han G Q, Jiang X W, Liu Y, Zhang J C, Hao Y 2019 IEEE Trans. Electron Devices 66 1985

[5] Wang P C, Huang P R, Ghosh S, Bansal R, Jheng Y T, Lee K C, Cheng H H, Chang G E 2024 ACS Photonics 11 2659
[6] Reboud V, Concepción O, Du W, El Kurdi M, Hartmann J M, Ikonic Z, Assali S, Pauc N, Calvo V, Cardoux C, Kroemer E, Coudurier N, Rodriguez P, Yu S Q, Buca D, Chelnokov A 2024 Photon. Nanostruc. Fundam. Appl. 58 101233
[7] Zheng J, Liu Z, Xue C L, Li C B, Zuo Y H, Cheng B W, Wang Q M 2018 J. Semicond. 39 061006
[8] Zhou Y Y, Dou W, Du W, Pham T, Ghetmiri S A, Al-Kabi S, Mosleh A, Alher M, Margetis J, Tolle J, Sun G, Soref R, Li B, Mortazavi M, Naseem H, Yu S Q 2016 J. Appl. Phys. 120 023102
[9] Ghetmiri S A, Du W, Margetis J, Mosleh A, Cousar L, Conley B R, Domulevicz L, Nazzal A, Sun G, Soref R A, Tolle J, Li B, Naseem H A, Yu S Q 2014 Appl. Phys. Lett. 105 151109
[10] Wirths S, Geiger R, von den Driesch N, Mussler G, Stoica T, Mantl S, Ikonic Z, Luysberg M, Chiussi S, Hartmann J M, Sigg H, Faist J, Buca D, Grützmacher D 2015 Nat. Photonics 9 88
[11] Arakawa Y, Nakamura T, Urino Y, Fujita T 2013 IEEE Commun. Mag. 51 72
[12] Wu S T, Zhang L, Wan R Q, Zhou H, Lee K H, Chen Q M, Huang Y C, Gong X, Tan C S 2023 Photonics Res. 11 1606
[13] Liu X Q, Zhang J, Niu C Q, Liu T R, Huang Q X, Li M M, Zhang D D, Pang Y Q, Liu Z, Zuo Y H, Cheng B W 2022 Photonics Res. 10 1567
[14] Ghosh S, Sun G, Yu S Q, Chang G E 2025 IEEE J. Sel. Top. Quantum Electron. 31 1
[15] Huang S H, Xie W M, Wang H C, Lin G Y, Wang J Q, Huang W, Li C 2018 Acta Phys. Sin. 67 040501
[16] Huang S H, Zheng Q Q, Xie W M, Lin J Y, Huang W, Li C, Qi D F 2018 J. Phys. Condens. Matter 30 465701
[17] Murphy-Armando F, Murray É D, Savić I, Trigo M, Reis D A, Fahy S 2023 Appl. Phys. Lett. 122 012202
[18] Wang C, Wang H, Chen W, Xie X, Zong J, Liu L, Jin S, Zhang Y, Yu F, Meng Q, Tian Q, Wang L, Ren W, Li F, Zhang H, Zhang Y 2021 Nano Lett. 21 8258
[19] Stern M J, René de Cotret L P, Otto M R, Chatelain R P, Boisvert J P, Sutton M, Siwick B J 2018 Phys. Rev. B 97 165416
[20] Huang P, Zhang Y, Hu K, Qi J, Zhang D, Cheng L 2024 Chin. Phys. B 33 017201
[21] Rogowicz E, Kopaczek J, Kutrowska-Girzycka J, Myronov M, Kudrawiec R, Syperek M 2021 ACS Appl. Electron. Mater. 3 344
[22]Rideau D, Feraille M, Ciampolini L, Minondo M, Tavernier C, Jaouen H, Ghetti A 2006 Phys. Rev. B 74 195208
[23] Song Z, Fan W, Tan C S, Wang Q, Nam D, Zhang D H, Sun G 2019 New J. Phys. 21 073037
[24] Lever L, Ikonić Z, Valavanis A, Kelsall R W, Myronov M, Leadley D R, Hu Y, Owens N, Gardes F Y, Reed G T 2012 J. Appl. Phys. 112 123105
[25] Liu S Q, Yen S T 2019 J. Appl. Phys. 125 245701
[26] Wang X, Li H, Camacho-Aguilera R, Cai Y, Kimerling L C, Michel J, Liu J 2013 Opt. Lett. 38 652
[27] Claussen S A, Tasyurek E, Roth J E, Miller D A B 2010 Opt. Express 18 25596
[28] Zhou X Q, van Driel H M, Mak G 1994 Phys. Rev. B 50 5226
[29] Mak G, van Driel H M 1994 Phys. Rev. B 49 16817